We are IntechOpen, the world's leading publisher of Open Access books Built by scientists, for scientists

4,800
Open access books available

122,000
International authors and editors

135M
Downloads

Our authors are among the

154
Countries delivered to

TOP 1%
most cited scientists

12.2%
Contributors from top 500 universities

CLARIVATE ANALYTICS
BOOK CITATION INDEX
INDEXED

WEB OF SCIENCE™

Selection of our books indexed in the Book Citation Index
in Web of Science™ Core Collection (BKCI)

Interested in publishing with us?
Contact book.department@intechopen.com

Numbers displayed above are based on latest data collected.
For more information visit www.intechopen.com

Spatial Modulation – A Low Complexity Modulation Technique for Visible Light Communications

Hammed G. Olanrewaju,

Funmilayo B. Ogunkoya and Wasiu O. Popoola

Additional information is available at the end of the chapter

Abstract

In visible light communication (VLC), the fundamental limitation on the achievable data rate/spectral efficiency is imposed by the optical source, particularly the phosphor-converted white light emitting diode (LED). These low-cost white LEDs favoured in solid-state lighting have very limited modulation bandwidth of less than 5 MHz, typically. This imposes a severe limitation on the attainable data rate. This is recognised in the literature and has led to the emergence of techniques such as multiple-input-multiple-output (MIMO) VLC systems as a means of addressing this challenge. The MIMO approach takes advantage of the multi-LED/multi-receiver structure to improve performance. In this chapter, we shall be discussing spatial modulation (SM) as a novel low-complexity MIMO technique for the VLC system. The SM technique exploits the spatial location of the individual LED as an additional degree of freedom in data modulation. Moreover, the chapter includes the comparison analysis of the SM technique with other traditional methods of modulation such as on-off keying (OOK) and pulse position modulation (PPM).

Keywords: spatial modulation, optical wireless communication, visible light communication, space shift keying

1. Introduction

The need for high data rate transmission to meet the demands of existing and emerging data-intensive applications and services is one of the key elements driving the research in the area of wireless communications access technology. Visible light communication (VLC) system, with its significantly large inherent optical spectrum, is a promising technology capable of delivering high data rates. However, one of its major drawbacks is the limited modulation

bandwidth of light emitting diodes (LEDs). This limitation prevents some of the conventional wireless modulation techniques from fully exploiting the huge optical spectrum in achieving high-speed communications. To fully utilise the inherent resources of VLC while mitigating the effects of this limitation, a multiple-input multiple-output (MIMO) access technique such as spatial modulation (SM) is an attractive option.

SM technique in VLC facilitates efficient management of the limited LED modulation bandwidth in a power-efficient manner without sacrificing the complexity of the system. A study in Ref. [1] proposed SM for optical wireless systems using the same principle of SM for a radio frequency (RF) system [2]. One of the interesting features of VLC is the possibility of the system to serve a dual function of data transmission by intensity-modulating LEDs alongside their primary purpose of illumination. In practice, an LED luminaire usually has multiple LEDs used for illumination due to the limited luminous flux of an individual LED. Thus, SM leverages the spatial dimensions of these multiple LEDs as an additional degree of freedom for high data rate transmission [1]. The information sequence to be transmitted is mapped to symbols chosen from the signal constellation points of a digital modulation technique. The fundamental concept of SM relies on these spatially separated LEDs considered as spatial constellation points, which are utilised to convey additional information bits [3]. During a symbol duration, the transmit bits are mapped to one of the spatial constellation points, thereby activating one transmit unit only at a particular time instance. The strength of channel correlation between the transmit-receive unit plays a significant role in the performance of the SM technique. Hence, there is a need for intensive research on performance enhancement schemes of SM.

Various optical SM techniques in VLC reported in the literature to enhance the data rate include spatial pulse position modulation (SPPM) proposed in Ref. [4], where a combination of space shift keying (SSK) and pulse position modulation (PPM) is considered. The idea was later generalised in Ref. [5] by activating multiple LEDs during each symbol's duration in order to increase the number of bits transmitted at a time instance. The use of optical space shift keying (OSSK) [6], spatial pulse amplitude modulation (S-PAM) [7], and generalised space shift keying (GSSK) [8] to boost VLC spectral efficiency using SM has equally been investigated.

The focus of this chapter is to address the error performance challenges of SM in VLC. A detailed description of the conventional SM and different variants of SM is presented. Analytical expressions for the error performance evaluations of these variants are derived in the presence of VLC channel impairments and additive white Gaussian noise (AWGN). These solutions are compared with computer-based simulations to validate the closed-form expressions. Furthermore, the attainable data rate using SM is quantified by comparing the spectral efficiency of SM with the classical modulation techniques such as on-off keying (OOK) and PPM.

2. Principle of optical spatial modulation

2.1. Generation and detection

In a VLC system with N_t LED transmitting unit and N_r receivers (photodetectors (PD)), using optical SM technique, only one of the LEDs is active during any symbol duration while the

rest of the LEDs is idle. For applications in VLC, an idle LED is driven by only the DC bias required to turn on the LED for illumination, while the active LED is driven by the sum of the DC bias and a current swing whose magnitude is dependent on the digital signal modulation imposed on the optical carrier. At the transmitter, the information bits to be transmitted are grouped into data symbols, and the block of information bits in each data symbol is mapped onto two information carrying units, namely spatial and signal constellations points. The total number of bits transmitted per symbol is given by $M = \log_2(LN_t)$, where L denotes the number of the digital signal constellation points. The spatial modulator at the transmitter maps the first $\log_2(N_t)$ most significant bits of each symbol to the spatial constellation point, which is used to select the LED that will be active, while the remaining $\log_2(L)$ bits are mapped to the signal constellation point. The signal constellation point is conveyed by the transmitted digital signal modulation such as pulse amplitude modulation (PAM) [9], PPM [4], and orthogonal frequency division multiplexing (OFDM) [10], among others. For instance, if PAM is used for signal modulation, the signal constellation point determines the intensity level of the optical signal that will be emitted by the active LED. As an illustration, the encoding mechanism for an optical SM scheme with $N_t = 4$, $L = 4$, and $M = 4$ bits/symbol is shown in **Figure 1**. Considering the first data symbol which consists of bits '1101', LED 4 is selected to be activated based on the first two most significant bits, '11'. The remaining two bits, '01', are encoded in the signal constellation point 'S2'.

The signal emitted by the active LED propagates through the optical wireless channel. At the receiving end, the radiated signal is detected by one or more PDs. The channel condition of each transmitter-receiver path is described by the channel impulse response $h(t)$, and this is typically fixed for a specified configuration of the transmitter, receiver, and any intervening reflectors [11]. Due to the differences in the spatial location of each LED, the optical signal emitted by each LED experiences different channel conditions. That is, the channel imprints a distinct signature on the signal emitted by a given LED, which makes it unique compared to the signal emitted by other LEDs. Considering an optical MIMO system realised through intensity modulation and direct detection (IM/DD), assuming line-of-sight (LOS) paths
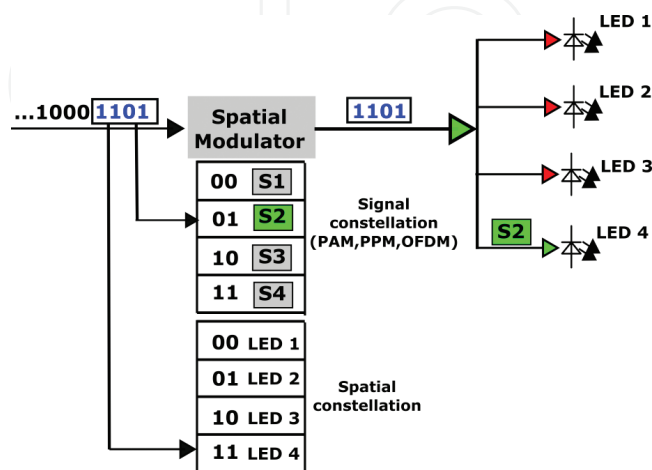

Figure 1. An illustration of the encoding mechanism of an optical SM technique.

between the transmitters and the receivers, with negligible temporal delay [7], the $N_r \times N_t$ optical MIMO channel's gain matrix $\mathbf{H}$ is given by:

$$\mathbf{H} = \begin{bmatrix} h_{11} & h_{12} & \cdots & h_{1N_t} \\ h_{21} & h_{22} & \cdots & h_{2N_r} \\ \vdots & \vdots & \ddots & \vdots \\ h_{N_r1} & h_{N_r2} & \cdots & h_{N_rN_t} \end{bmatrix} \tag{1}$$

where h_{ij} is the channel's path gain between the i-th PD and the j-th LED. Using the baseband channel model for the VLC system, ($N_r \times 1$)-dimensional vector of the received electrical signal can be expressed as:

$$\mathbf{r}(t) = R\mathbf{Hs}(t) + \mathbf{n}(t), \tag{2}$$

where R is the responsivity of the PD, and $\mathbf{s}(t)$ is the ($N_t \times 1$)-dimensional vector of the transmitted signal. The noise vector $\mathbf{n}(t)$ is the sum of receiver thermal noise and ambient light shot noise; it is usually modelled as independent and identically distributed AWGN.

At the receiver, the detector exploits the uniqueness of the channel condition associated with each transmit-receive channel path to estimate the transmitted data symbol. Thus, a prior knowledge of channel impulse response (CIR) of all the transmit-receive paths is required at the receiver. In practice, the CIR can be obtained through channel estimation technique. According to the maximum likelihood (ML) criterion, the detector computes the Euclidean distance between the received signal and the set of possible signals from all the LN_t combinations of LED index and digital signal modulation index and decides in favour of the combination associated with the smallest Euclidean distance. The estimate of the transmitted signal is obtained as:

$$\hat{\mathbf{S}} = \arg\ \min_{\mathbf{s} \in \mathbb{S}} \|\mathbf{r} - R\mathbf{Hs}\|^2, \tag{3}$$

where $\mathbb{S}$ is the set of all possible LN_t signals.

2.2. Variants of optical spatial modulation

Due to its promising potentials as highlighted in Section 1, SM has been implemented for VLC systems in various forms. Differences in these variants include, but are not limited to, the inclusion or exclusion of digital signal modulation, the type of digital signal modulation employed, and the number of optical sources that are activated concurrently. Brief descriptions of some reported variants of optical SM are provided as follows.

Optical space shift keying (OSSK): This is a class of optical SM technique, which does not involve the use of digital signal modulation scheme. The source information is encoded solely on the spatial position of the LEDs. As in the conventional optical SM described above, OSSK activates a single LED in a given symbol duration. The total number of bits transmitted per symbol in OSSK is $\log_2(N_t)$. Due to the absence of digital signal modulation, the transceiver requirement such as synchronisation is reduced, and the detection complexity at the receiver is lowered [12]. However, the drawback of not using signal modulation in OSSK is that the achieved

transmission rate is lower than conventional SM schemes. This limitation can be addressed by adding signal modulation and/or employing a large array of optical sources and activating multiple sources concurrently. An illustration of OSSK modulation scheme with four LEDs is depicted in **Figure 2**. Two information bits are transmitted per SSK symbol, and the first two bits, '01', are transmitted by activating LED 2.

Generalised spatial shift keying (GSSK): In GSSK, multiple LEDs can be activated during a symbol duration, and information on the transmitted symbol is encoded solely on the indices of the activated LEDs. As in OSSK, signal modulation is not used in GSSK. The GSSK modulation scheme can be implemented by activating a fixed number of sources, N_a, $(1 < N_a < N_t)$ in any symbol duration and varying the indices of the activated sources based on the bits contained in the symbol to be transmitted [13]. The scheme can also be implemented by varying both the number and the indices of the activated sources based on bits of the data symbol to be transmitted [8, 14, 15]. Considering the latter implementation of GSSK, a total of N_t bits are transmitted per data symbol as against $\log_2 (N_t)$ in OSSK. As described in Ref. [8], the number and position of ones (1s) in the bits of the symbol to be transmitted determine the number and the indices of the LEDs that will be activated. During a symbol duration, each activated LED transmits a return-to-zero (RZ) pulse of fixed but predefined width and a peak power P_t. For any data symbol with N_t data bits, except when all the bits are zero, the LEDs whose positions correspond to the bit value one are activated to transmit a pulse with duty cycle τ, while all the other LEDs are idle, where $0 < \tau \leq 1$. However, when the data bits are all zero, all the LEDs are activated, but they transmit a pulse with duty cycle $(1 - \tau)$. As an illustration, the pulse pattern for a 2-LED GSSK scheme is shown in **Figure 3**.

Spatial pulse position modulation (SPPM): This is an optical SM scheme that combines SSK with PPM [4]. In SPPM, only one LED is activated to transmit optical data signal in any given symbol duration, and the activated LED transmits an L-PPM pulse pattern, where L is the number of PPM time slots in a symbol duration. By combining SSK with PPM in SPPM, the spectral efficiency of PPM can be improved while still retaining its energy efficiency. In SPPM scheme, a total of $\log_2 (LN_t)$ bits are transmitted per symbol. The SPPM scheme is illustrated in **Figure 4** for the case of $N_t = 4$, $L = 2$, and $M = 3$ bits/symbol. The two most significant bits of each symbol determine the index of the LED that will be activated while the last bit determines
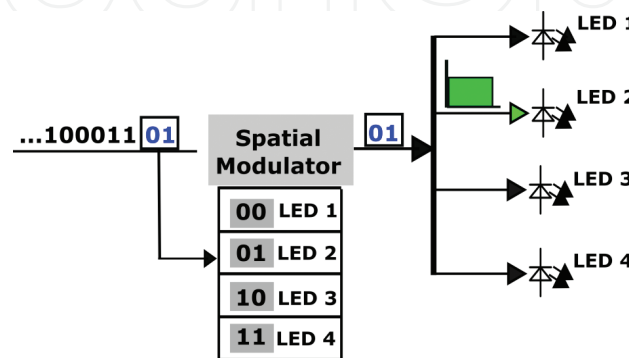

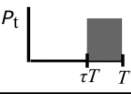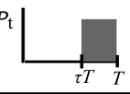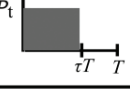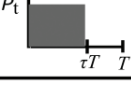**Figure 2.** An illustration of OSSK modulation using four LEDs.
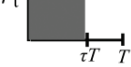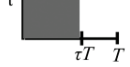
Figure 3. An illustration of the pulse pattern for GSSK scheme using two LEDs.
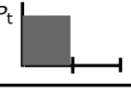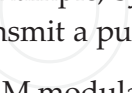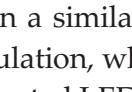
Figure 4. An illustration of intensity modulation for SPPM scheme using four LEDs.

the pulse position in the PPM pulse pattern. As an example, symbol '3' with binary representation '011' is transmitted by activating LED 2 to transmit a pulse in the second time slot.

Spatial pulse amplitude modulation (S-PAM): S-PAM modulation scheme combines SSK and PAM. The encoding mechanism in S-PAM is done in a similar fashion to SPPM. The S-PAM scheme employs a K-PAM scheme for its signal modulation, where K represents the number of optical intensity levels that can be emitted by the activated LED. For instance, the k-th intensity level can be defined as [7]:

$$I_k = \frac{2kI}{K+1}, \text{ for } k = 1, \ldots, K;$$

(4)

where I is the mean emitted optical power. A total of $\log_2(LK)$ bits are transmitted during each symbol duration, where the first $\log_2(N_t)$ most significant bits of each symbol determine the

index of the LED that will be activated while the remaining $\log_2(K)$ is used to determine the intensity level of the emitted optical radiation.

Generalised spatial modulation (GSM): Like the generalisation of SSK to GSSK, SM schemes can be generalised by activating multiple LEDs in each symbol duration and making each activated LED transmit the same or different digital signal modulation. Such schemes are referred to as generalised spatial modulation (GSM) [5, 16–18]. GSM offers spectral efficiency gain by increasing the number of bits transmitted during each symbol duration. For instance, the GSSK scheme described above can be combined with PPM to develop a generalised SPPM (GSPPM) scheme [5] with a total number of $N_t + \log_2(L)$ bit/symbol. The active sources must, however, be synchronised to avoid inter-symbol interference (ISI).

In the GSPPM scheme [5], during a given symbol duration, one or more LEDs can be activated to concurrently transmit the same L-PPM pulse pattern. The most significant N_t bits of each symbol constitute the spatial constellation point, which determines the indices of the activated LEDs, while the remaining $\log_2 (L)$ bits make up the signal constellation point, which is conveyed by the position of the pulse in PPM signal. LED activation in GSPPM is done in a similar fashion to the GSSK scheme, albeit with a slight modification. That is, the number of ones (1s) in the spatial constellation point determines the number and the indices of the active LEDs, but pulse inversion (PI) technique is employed in GSPPM instead of the RZ pulses used in GSSK. The PI technique entails using bipolar pulses such that for all spatial constellation points, except when all the bits that constitute the spatial constellation are zeros, the activated LEDs are driven with electrical pulse signals of amplitude V volts. When all the bits that constitute spatial constellations are zeros, all the LEDs are activated, but they are driven with an electrical pulse signal of amplitude $-V$ volts. By using bipolar pulses, GSPPM requires a DC bias to convert the negative pulses to positive voltages required in IM/DD VLC. Although this implies additional power consumption, however, for applications in VLC, this may not be a drawback since DC bias will be required when the LEDs are used for illumination. The GSPPM scheme is further illustrated in **Figure 5**, for the case of $N_t = 2$ and $L = 2$. As an example, to transmit
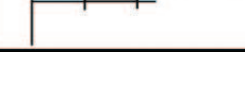
Data symbol	Binary equivalent	Spatial Constellation	Signal Constellation	Activated LEDs	Sample PPM Signal Pattern
0	000	00	0	1 and 2	[000] -V
1	001	00	1		
2	010	01	0	1	[011] V
3	011	01	1		
4	100	10	0	2	[100] V
5	101	10	1		
6	110	11	0	1 and 2	[111] V
7	111	11	1		

Figure 5. An illustration of GSPPM scheme.

symbol '1', with binary equivalent '001', because the first two bits which are used to select the spatial constellation point are both zeros, the two LEDs are activated and are driven by −V volts while the last bit of the symbol, '1', indicates that the pulse be transmitted in the second time slot.

2.3. Contrast with spatial multiplexing, spatial diversity, and repetition coding

Beside SM, other MIMO transmission techniques that have been considered for VLC include repetitive coding (RC) and spatial multiplexing (SMP). In RC, the same information is simultaneously transmitted from all the transmitters, and the transmitted signals add up constructively at the receiver. In essence, RC offers diversity gain, which makes it more robust to channel the correlation compared to SMP and SM. However, since RC does not provide spatial multiplexing gains, large signal constellation sizes will be required to achieve high spectral efficiency. In contrast, SMP enables high data rates by transmitting different kinds of information from each transmitter. The drawback of SMP is that it requires sufficiently low channel correlation. SM is more robust to correlated channels compared to SMP, and it provides larger spectral efficiency compared to RC [7].

In terms of complexity, the optical SM constitutes a low complexity technique of increasing the achievable transmission rates in VLC systems. Compared to other spectrally efficient modulation schemes like the optical OFDM [19] and PAM, the SM technique is not as sensitive to nonlinearity effects of the system components [4, 20]. Hence, SM-based VLC systems do not require the complex pre-distortion algorithm to compensate for device nonlinearity. Moreover, since only one or a few LED(s) is active in each symbol duration, inter-channel interference (ICI), which results from multiple and concurrent signal transmission, is reduced in optical SM as compared to RC and SMP. Hence, receiver design is made simpler and ML-optimum performance can be achieved at a reduced decoding complexity [21].

The computational complexity of the ML-based detection of optical S-PAM is compared with that of RC and SMP in **Table 1** [22]. The computational complexity is defined as the total number of required mathematical operations, that is, multiplications, additions, and subtractions that are required for ML detection. **Table 1** shows that, to achieve equal spectral efficiency, the detection of SM is less computationally intensive compared to RC and SMP. Because SM conveys additional bits via the spatial domain, it employs a smaller digital signal constellation size to achieve the same spectral efficiency as RC.

MIMO technique	Number of mathematical operations at the receiver
RC	$L(2N_tN_r + N_r - 1)$
SMP	$L^{N_t}(2N_tN_r + N_r - 1)$
SM	$LN_t(3N_r - 1)$

L denotes the size of digital signal constellation.

Table 1. Computational complexity at the receiver of RC, SMP, and SM techniques [22].

3. Error performance of optical spatial modulation

In this section, the error performance of four variants of optical SM technique is analysed and closed-form expressions for their symbol error are derived. These expressions are validated using Monte-Carlo simulations. The optical SM variants considered are SPPM, OSSK, GSSK, and GSPPM. In the following, without any loss of generality, a MIMO VLC system, $N_t = 4$ and $N_r = 2$, is considered. The LOS channel gain matrix, **H**, is obtained from the simulated indoor optical channel, which is performed based on the ray-tracing algorithm in Ref. [23]. The normalised LOS channel matrix is obtained as:

$$\mathbf{H} = \begin{bmatrix} 1 & 0.3118 & 0.2496 & 0.1283 \\ 1 & 0.3925 & 0.2709 & 0.1578 \end{bmatrix} \tag{5}$$

3.1. Error performance analysis of SPPM

As described in Section 2.2, the data symbol in SPPM is conveyed by the index of the active LED and the pulse position of the transmitted PPM signal. These two parameters must be estimated at the receiver in order to demodulate the transmitted symbol. Hence, error performance analysis will involve evaluating the probability of the correct pulse position and LED index detection. Considering that an SPPM symbol is transmitted by activating the j-th LED to transmit a pulse in the m-th PPM time slot, the transmit signal vector $\mathbf{s}_j^m(t)$ can be expressed as:

$$\mathbf{s}_j^m(t) = [0, \cdots, x_j^m(t), \cdots, 0]^\mathsf{T}. \tag{6}$$

The nonzero entry, $x_j^m(\mathrm{t})$, positioned at the index of the active j-th LED, is the L-PPM signal imposed on the optical carrier emitted by the active LED. Without loss of generality, using rectangular pulse shaping, the L-PPM signal with amplitude P_t can be defined by:

$$x_j^m(t) = \begin{cases} P_t; & \text{for} (m-1)T_c \le t \le mT_c \\ 0; & \text{elsewhere} \end{cases} \tag{7}$$

where $T_c = T/L$ is the duration of each PPM time slot and T is the symbol duration. The receivers employ a unit energy receive filter, $f_c(t)$, which is matched to the PPM waveform and is given by:

$$f_c(t) = \frac{1}{\sqrt{T_c}} \mathrm{rect}\left(\frac{t - T_c/2}{T_c}\right). \tag{8}$$

where $\mathrm{rect}(x) = 1$ for $|x| < 1/2$. The outputs of the matched filters (MF) are sampled at the rate $1/T_c$ to obtain the samples of each PPM time slot. For N_r PDs and L-PPM, the $N_r \times L$ array of the outputs of the matched filters in each time slot and for all PDs can be expressed as:

$$\begin{aligned} \mathbf{Y} &= \mathbf{X}_j^m + \mathbf{N} \\ &= [\mathbf{0} \quad \cdots \mathbf{h}_j \sqrt{E_S^{\mathrm{SPPM}}} \cdots \mathbf{0}] + [\mathbf{n}_1 \quad \cdots \mathbf{n}_m \cdots \mathbf{n}_L] \\ &= [\mathbf{y}_1, \quad \cdots \mathbf{y}_{m'} \cdots \mathbf{y}_L] \end{aligned} \tag{9}$$

where $\mathbf{X}_j^m$ is the $(N_{\mathrm{r}} \times L)$-dimensional array of the samples of noiseless matched filter output and $\mathbf{N}$ is the Gaussian noise at the output of the matched filter with variance $\sigma_{\mathrm{n}}^2 = N_0/2$. $E_{\mathrm{s}}^{\mathrm{SPPM}} = (RP_{\mathrm{t}})^2 T_{\mathrm{c}}$ is the transmit energy of the SPPM symbol. The column vector $\mathbf{h}_j$ represents the channel gain from the j-th LED to all the PDs, that is, the j-th column of the channel matrix $\mathbf{H}$. Using ML detection criterion, the estimate of transmitted symbol, $\hat{a} = [\hat{m}, \hat{j}]$, is obtained as:

$$\hat{a} = [\hat{m}, \hat{j}] = \arg \max_{m,j} p(\mathbf{Y}|\,\mathbf{X}_j^m) \tag{10}$$

$$[\hat{m}, \hat{j}] = \arg \max_{m,j} D(\mathbf{Y}|\,\mathbf{X}_j^m) \tag{11}$$

The joint probability density function of $\mathbf{Y}$ conditioned on $\mathbf{X}_j^m$ is given by:

$$p(\mathbf{Y}|\,\mathbf{X}_j^m) = \frac{1}{(\pi N_0)^{LN_r/2}} \exp\left[-\frac{\|\mathbf{Y} - \mathbf{X}_j^m\|_F^2}{N_0}\right], \tag{12}$$

and the Euclidean distance metric $D(\mathbf{Y}, \mathbf{X}_j^m)$ is computed as:

$$D(\mathbf{Y}, \mathbf{X}_j^m) = \|\mathbf{Y} - \mathbf{X}_j^m\|_F^2 \tag{13}$$

where $\|\cdot\|_F$ denotes the Frobenius norm. The detection process entails obtaining the estimated pulse position, $\widehat{m}$, from:

$$\hat{m} = \arg \max_{\mathrm{m}} \left(\sum_i^{N_r} y_{i,\,m}\right), \tag{14}$$

and then estimating the index of the activated LED from the minimum Euclidean distance metric using the ML detection criterion.

Let the probability of a correctly decoded pulse position be defined by $P_{\mathrm{c,\,ppm}} = p(\hat{m} = m)$; then, the probability of correctly decoding the LED index given that the pulse position has been correctly decoded can be expressed as $P_{\mathrm{c,\,tx}} = p(\hat{j} = j\,|\,\hat{m} = m)$. Therefore, the probability of correct symbol detection is given by:

$$P_{\mathrm{c,\,sym}}^{\mathrm{SPPM}} = P_{\mathrm{c,\,tx}} \times P_{\mathrm{c,\,ppm}} = p(\hat{j} = j\,|\,\hat{m} = m) \times p(\hat{m} = m) \tag{15}$$

and the probability of symbol error is obtained as:

$$P_{\mathrm{e,\,sym}}^{\mathrm{SPPM}} = 1 - P_{\mathrm{c,\,sym}}^{\mathrm{SPPM}} = 1 - (P_{\mathrm{c,\,tx}} \times P_{\mathrm{c,\,ppm}}) \tag{16}$$

Probability of correctly detecting the index of the activated LED. To evaluate the probability of correctly decoding the LED index, we shall first find the pairwise error probabilities (PEP). Consider that the activated LED transmitted a pulse in slot m, the $\mathrm{PEP}_m^{j\to k}$, that the receiver decides in favour of LED k instead of LED j is given by:

$$\text{PEP}_m^{j \to k} = p\left(D(\mathbf{Y}, \mathbf{X}_j^m) > D(\mathbf{Y}, \mathbf{X}_k^m) \right) = p\left(\left\| \mathbf{y}_m - \mathbf{h}_j \sqrt{E_S^{\text{SPPM}}} \right\|_F^2 > \left\| \mathbf{y}_m - \mathbf{h}_k \sqrt{E_S^{\text{SPPM}}} \right\|_F^2 \right)$$

$$= Q\left(\|\mathbf{h}_j - \mathbf{h}_k\|_F \sqrt{\frac{E_S^{\text{SPPM}}}{2N_0}} \right) = Q\left(\|\mathbf{h}_j - \mathbf{h}_k\|_F \sqrt{\frac{\gamma_S^{\text{SPPM}}}{2}} \right) \tag{17}$$

where $Q(\cdot)$ denotes the Q-function, and $\gamma_S^{\text{SPPM}} = E_S^{\text{SPPM}}/N_0$ is the transmit signal-to-noise ratio (SNR) per SPPM symbol. For N_t equiprobable LEDs, the probability of error in decoding the index of the activated LED conditioned on a correctly decoded pulse position is obtained as:

$$P_{e,\,tx} = \frac{2}{N_t} \sum_{j=1}^{N_t-1} \sum_{k=j+1}^{N_t} \text{PEP}_m^{j \to k} = \frac{2}{N_t} \sum_{j=1}^{N_t-1} \sum_{k=j+1}^{N_t} Q\left(\|\mathbf{h}_j - \mathbf{h}_k\|_F \sqrt{\frac{\gamma_S^{\text{SPPM}}}{2}} \right), \tag{18}$$

and the probability of correctly decoding the index of the activated LED is computed as:

$$P_{c,\,tx} = 1 - \left[\frac{2}{N_t} \sum_{j=1}^{N_t-1} \sum_{k=j+1}^{N_t} Q\left(\|\mathbf{h}_j - \mathbf{h}_k\|_F \sqrt{\frac{\gamma_s^{\text{SPPM}}}{2}} \right) \right] \tag{19}$$

Probability of correctly detecting the transmitted pulse position. Given that the j-th LED is activated to transmit a pulse in slot m, then the $\text{PEP}_{m \to q}^j$ that the receiver decides in favour of slot q instead of slot m can be expressed as:

$$\text{PEP}_{m \to q}^j = p\left(\mathfrak{D}(\mathbf{Y}, \mathbf{X}_j^m) > D(\mathbf{Y}, \mathbf{X}_j^q) \right) \tag{20}$$

where,

$$\mathfrak{D}(\mathbf{Y}, \mathbf{X}_j^m) = \left\| \mathbf{y}_m - \mathbf{h}_j \sqrt{E_S^{\text{SPPM}}} \right\|_F^2 + (\mathbf{y}_q)^2 = (\mathbf{n}_m)^2 + (\mathbf{n}_q)^2 \tag{21}$$

$$\mathfrak{D}(\mathbf{Y}, \mathbf{X}_j^q) = (\mathbf{y}_m)^2 + \left\| \mathbf{y}_q - \mathbf{h}_j \sqrt{E_S^{\text{SPPM}}} \right\|_F^2 = \left\| \mathbf{h}_j \sqrt{E_S^{\text{SPPM}}} + \mathbf{n}_m \right\|_F^2 + \left\| \mathbf{n}_q - \mathbf{h}_j \sqrt{E_S^{\text{SPPM}}} \right\|_F^2 \tag{22}$$

Therefore,

$$\text{PEP}_{m \to q}^j = p\left((\mathbf{n}_q - \mathbf{n}_m)^\mathsf{T} \mathbf{h}_j > \sqrt{E_S^{\text{SPPM}}} \|\mathbf{h}_j\|_F^2 \right) = Q(\|\mathbf{h}_j\|_F \sqrt{\gamma_S^{\text{SPPM}}}). \tag{23}$$

For N_t equiprobable LEDs, the union bound technique [24] gives the probability of error in decoding the transmitted pulse position as:

$$P_{\text{e, ppm}} = \frac{1}{N_{\text{t}}} \sum_{j=1}^{N_{\text{t}}} \left((L-1) \times \text{PEP}_{m \to q}^{j} \right) = \frac{1}{N_{\text{t}}} \sum_{j=1}^{N_{\text{t}}} \left((L-1) \times Q(\|\mathbf{h}_j\|_{\text{F}} \sqrt{\gamma_{\text{S}}^{\text{SPPM}}}) \right) \qquad (24)$$

Thus, the average probability of correctly decoding the transmitted pulse position is:

$$P_{\text{c, ppm}} = 1 - \left[\frac{1}{N_t} \sum_{j=1}^{N_{\text{t}}} \left((L-1) \times Q\left(\|\mathbf{h}_j\|_{\text{F}} \sqrt{\gamma_{\text{S}}^{\text{SPPM}}} \right) \right) \right] \qquad (25)$$

By combining Eqs. (16), (19), and (25), the union bound on the average probability of symbol error of the SPPM scheme is derived as [4]:

$$P_{\text{e, sym}}^{\text{SPPM}} \leq 1 - \left[1 - \frac{2}{N_{\text{t}}} \sum_{j=1}^{N_{\text{t}}-1} \sum_{k=j+1}^{N_{\text{t}}} Q\left(\|\mathbf{h}_j - \mathbf{h}_k\|_{\text{F}} \sqrt{\frac{\gamma_{\text{S}}^{\text{SPPM}}}{2}} \right) \right]$$

$$\left[\frac{(L-1)}{N_{\text{t}}} \sum_{j=1}^{N_{\text{t}}} \left(\frac{1}{(L-1)} - Q(\|\mathbf{h}_j\|_{\text{F}} \sqrt{\gamma_{\text{S}}^{\text{SPPM}}}) \right) \right] \qquad (26)$$

The expression in Eq. (26) indicates that for a given SNR, the error performance of SPPM strongly depends on the individual channel path gain of each transmitter-receiver link as well as the difference between these channel gain values. The error performance plots for different system configurations are shown in **Figure 6**. For the case of $N_{\text{r}} = 1$, $N_{\text{t}} = [2, 4]$, and $L = [2, 8]$, the achieved symbol error rate (SER) is plotted against the SNR per bit $\gamma_{\text{b}} = \gamma_{\text{s}}/M$. To validate the analysis, simulation results are also included. **Figure 6** shows that the analytical bound in Eq. (26) agrees with the simulation results. The slight deviation observed at SER $> 10^{-2}$ is due to the union bound techniques used in the analysis.

Moreover, as L increased from 2 to 8, the γ_{b} required to achieve an SER of 10^{-6} reduced by about 2 dB for $N_{\text{t}} = [2, 4]$. This shows the energy efficiency benefit that PPM adds to SPPM. Using more LEDs results in higher attainable data rate, but this requires distinct channel gains for all the LEDs and higher SNR. This explains why using two LEDs require up to about 16 dB less in SNR than using four LEDs, as shown in **Figure 6**.

3.2. Error performance analysis of OSSK

Using the description of the OSSK scheme provided in Section 2.2, OSSK can be viewed as a subset of SPPM scheme in which $L = 1$, and $T_c = T$. The transmitted symbol in SSK is determined by simply estimating the index of the activated LED. Therefore, the error performance analysis of OSSK is equivalent to the process of evaluating the probability of error in detecting the active LED in SPPM. By using $L = 1$ in the formulation of the error performance analysis of SPPM, the union bound on the average probability of symbol error of the SSK modulation scheme is obtained as:

$$P_{\text{e, sym}}^{\text{SSK}} \le \frac{2}{N_{\text{t}}} \sum_{j=1}^{N_{\text{t}}-1} \sum_{k=j+1}^{N_{\text{t}}} Q\left(\|\mathbf{h}_j - \mathbf{h}_k\|_{\text{F}} \sqrt{\frac{\gamma_{\text{S}}^{\text{SSK}}}{2}}\right) \qquad (27)$$

where $\gamma_{\text{s}}^{\text{SSK}} = E_{\text{s}}^{\text{SSK}}/N_0$ is the transmit SNR per SSK symbol. $E_{\text{s}}^{\text{SSK}} = (RP_{\text{t}})^2 T$ is the transmit energy per symbol. Note that Eq. (27) is the same as Eq. (18), and it can also be obtained by simply substituting $L = 1$ in Eq. (26). This conforms with our description of OSSK as being equivalent to an SPPM scheme with $L = 1$.

Using the closed-form expression in Eq. (27), the SER of OSSK is plotted against the SNR per bit γ_{b} in **Figure 7**. The plot shows a very tight match between the simulation and the theoretical analysis. It can be observed that at an SER of 10^{-6}, compared to $N_{\text{r}} = 1$, using $N_{\text{r}} = 2$ provides an SNR gain of about 2.5 and 7 dB for $N_{\text{t}} = 2$ and $N_{\text{r}} = 4$, respectively. This implies that the dependency of optical SM on decorrelated channel can be relaxed by using multiple PDs.

3.3. Error performance analysis of GSSK

According to the GSSK scheme described in Section 2.2, during a symbol duration, the number and the indices of the active LEDs are determined by the bits of the data symbol to be transmitted. Using N_{t} LEDs, there are $2^{N_{\text{t}}}$ possible GSSK symbols. Considering a single symbol duration, T, in which symbol v, for $v = 0, \ldots, (2^{N_{\text{t}}} - 1)$, is transmitted, the $(N_{\text{t}} \times 1)$-dimensional vector of the transmitted signal, $\mathbf{s}(t)$, can be expressed as $\mathbf{s}(t) = \tau P_{\text{t}} \mathbf{a}_v$, where $\mathbf{a}_v = [a_1, \ldots, a_{N_{\text{t}}}]^{\text{T}}$ is the LED activation vector for symbol v, and τ is the duty cycle of the transmitted optical pulse as explained in Section 2.2. The entries of $\mathbf{a}_v$ are binary digits, with
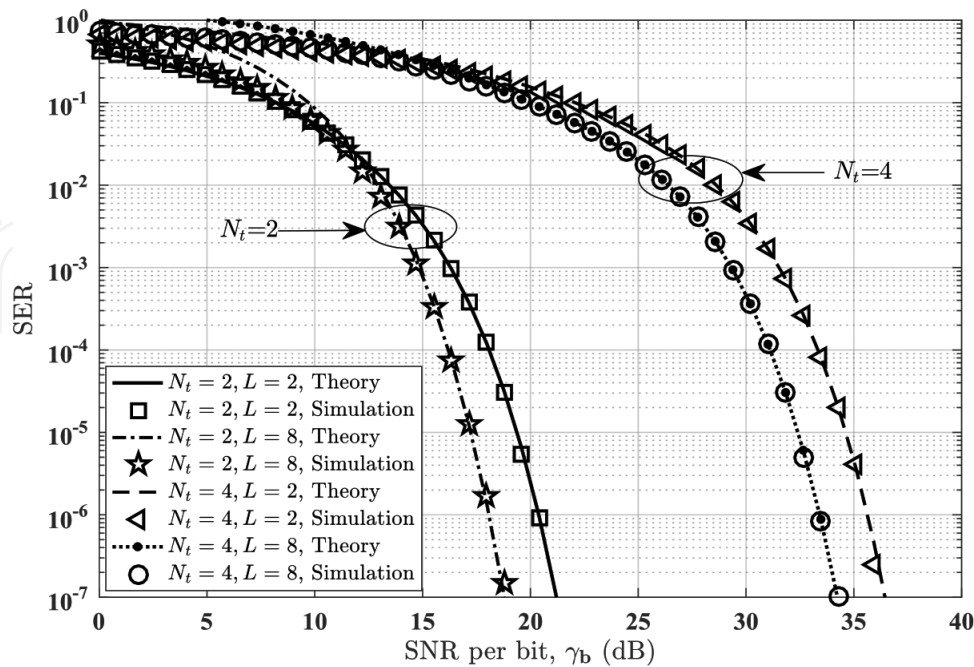

Figure 6. Error performance plot of SPPM for $N_{\text{t}} = [2,4]$, $N_{\text{r}} = 1$, and $L = [2, 8]$.
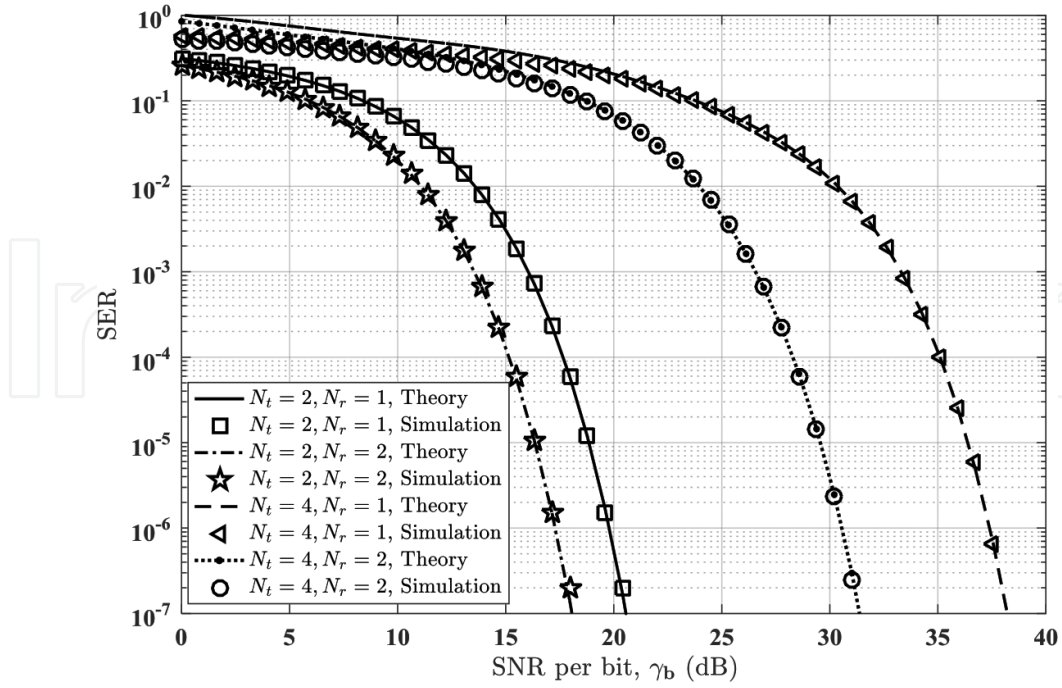
Figure 7. Error performance plot of OSSK for N_t = [2, 4] and N_r = [1, 2].

'1s' as the indices of activated LEDs and '0s' as the indices of the idle LEDs. The $(N_r \times 1)$-dimensional vector of the received electrical signal, $\mathbf{r}(t)$, is given by:

$$\mathbf{r}(t) = \tau R P_t \mathbf{H} \mathbf{a}_v + \mathbf{n}(t), \text{ for } 0 < t < T. \tag{28}$$

For tractability, $\mathbf{w}_v \triangleq \mathbf{H} \mathbf{a}_v$ is defined as the vector of the channel gains associated with the transmission of the GSSK symbol v. Hence,

$$\mathbf{r}(t) = \tau R P_t \mathbf{w}_v + \mathbf{n}(t), \text{ for } 0 < t < T. \tag{29}$$

As an illustration, considering a 2-LED GSSK system with N_r PDs, the received signal for all possible GSSK symbols is obtained as shown in **Table 2**. To estimate the transmitted symbol, the output of the matched filter, sampled at the rate $1/T$, is given by:

$$\mathbf{y} = \mathbf{x}_v + \mathbf{n} \tag{30}$$

where $\mathbf{x}_v = \mathbf{w}_v \sqrt{E_S^{GSSK}}$ and energy per symbol $E_S^{GSSK} = (R P_t)^2 \tau T$. Considering that GSSK symbol v is transmitted, the pairwise error probabilities, $\text{PEP}^{v \rightarrow u}$, that the receiver decides in favour of symbol u instead of symbol v are expressed as:

v	Binary equivalent	Activated LED	$\mathbf{w}_v$	$\mathbf{r}(t)$
0	00	LED 1 and LED 2	$\mathbf{h}_1 + \mathbf{h}_2$	$(1 - \tau) R P_t (\mathbf{h}_1 + \mathbf{h}_2) + \mathbf{n}(t)$
1	01	LED 1	$\mathbf{h}_1$	$\tau R P_t \mathbf{h}_1 + \mathbf{n}(t)$
2	10	LED 2	$\mathbf{h}_2$	$\tau R P_t \mathbf{h}_2 + \mathbf{n}(t)$
3	11	LED 1 and LED 2	$\mathbf{h}_1 + \mathbf{h}_2$	$\tau R P_t (\mathbf{h}_1 + \mathbf{h}_2) + \mathbf{n}(t)$

Table 2. LED activation for GSSK modulation using two LEDs.

$$\text{PEP}^{v \to u} = p\Big(D(\mathbf{y}, \mathbf{x}_v) > D(\mathbf{y}, \mathbf{x}_u)\Big)$$

$$= p\left(\left\|\mathbf{y} - \mathbf{w}_v \sqrt{E_S^{\text{GSSK}}}\right\|_F^2 > \left\|\mathbf{y} - \mathbf{w}_u \sqrt{E_S^{\text{GSSK}}}\right\|_F^2\right) \tag{31}$$

$$= Q\left(\|\mathbf{w}_v - \mathbf{w}_u\|_F \sqrt{\frac{E_S^{\text{GSSK}}}{2N_0}}\right) = Q\left(\|\mathbf{w}_v - \mathbf{w}_u\|_F \sqrt{\frac{\gamma_S^{\text{GSSK}}}{2}}\right).$$

where $\gamma_s^{\text{GSSK}} = E_s^{\text{GSSK}}/N_0$ is the transmit SNR per GSSK symbol. For 2^{N_t} equiprobable GSSK symbols, the union bound on the probability of symbol error of GSSK modulation is given by [8]:

$$P_{e,\,\text{sym}}^{\text{GSSK}} \leq \frac{2}{2^{N_t}} \sum_{v=1}^{2^{N_t}-1} \sum_{u=v+1}^{2^{N_t}} \text{PEP}^{v \to u} = \frac{2}{2^{N_t}} \sum_{v=1}^{2^{N_t}-1} \sum_{u=v+1}^{2^{N_t}} Q\left(\|\mathbf{w}_v - \mathbf{w}_u\|_F \sqrt{\frac{\gamma_S^{\text{GSSK}}}{2}}\right). \tag{32}$$

Without loss of generality, using $\tau = 1$, the closed-form expression derived for the SER of GSSK in Eq. (32) is validated by tightly matched simulation results as depicted by the error performance plots in **Figure 8** for the cases $N_t = [2,4]$ and $N_r = [1,2]$.

3.4. Error performance analysis of GSPPM

The performance analysis of GSPPM scheme entails combining the detection process in GSSK with the pulse position detection in SPPM. The transmitted symbol consists of the spatial constellation point, which determines the active LED and the pulse position of the transmitted PPM signal. Let λ denote pulse inversion constant associated with each spatial constellation point; $\lambda = -1$ if all the bits that constitute the spatial constellation point of the data symbol are zeros and otherwise $\lambda = +1$. Considering a single symbol duration, if the active LEDs transmit a pulse in the m-th time slot, the $(N_r \times 1)$-dimensional vector of the received electrical signal is given by:

$$\mathbf{r}(t) = \Big(R\lambda_v x_j^m(t)\Big)\mathbf{w}_v + \mathbf{n}(t), \text{ for } 0 < t < T. \tag{33}$$

where v denotes the spatial constellation point of the transmitted symbol. Other variables are as defined previously. As an illustration, considering a two-LED GSPPM system, the signal received in the pulse position of the transmitted PPM signal is obtained as shown in **Table 3**.

The error performance analysis will involve evaluating the probability of correctly estimating the spatial constellation point and the pulse position. The detection of the transmitted spatial constellation in GSPPM is equivalent to the detection of the transmitted GSSK symbol in Section 3.3. Hence, the probability of correctly detecting the transmitted spatial constellation is obtained as [5]:

$$P_{c,\,\text{scp}} \leq 1 - \frac{2}{2^{N_t}} \sum_{v=1}^{2^{N_t}-1} \sum_{u=v+1}^{2^{N_t}} Q\left(\|\lambda_v \mathbf{w}_v - \lambda_u \mathbf{w}_u\|_F \sqrt{\frac{\gamma_S^{\text{GSPPM}}}{2}}\right) \tag{34}$$
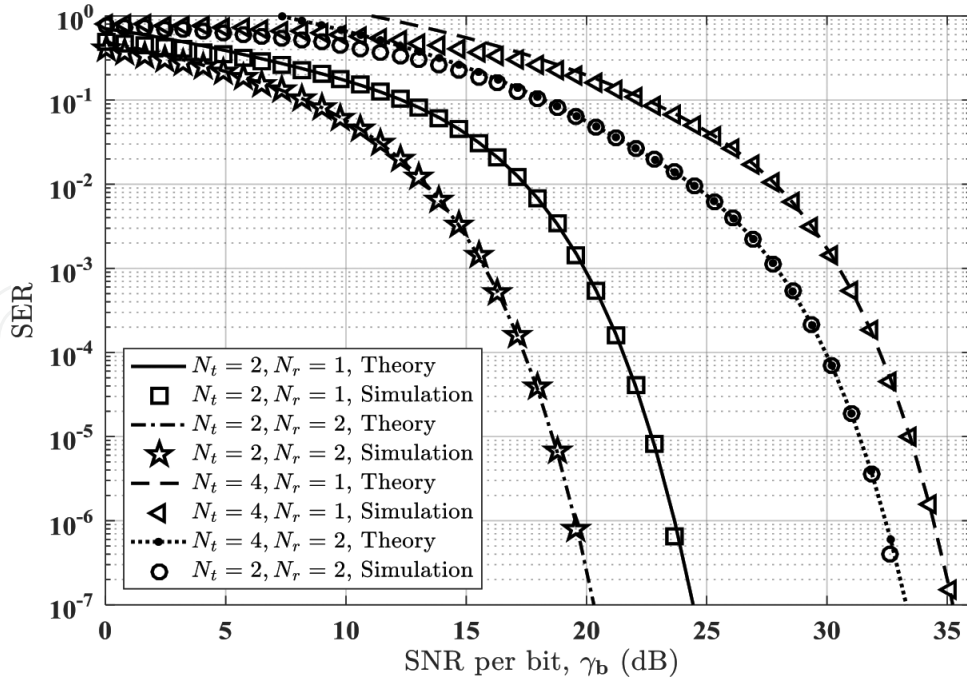
Figure 8. Error performance plot of GSSK for N_t = [2, 4] and N_r = [1, 2].

Spatial constellation	Activated LED	$\mathbf{w}_v$	λ_v	$\mathbf{r(t)}$
00	LED 1 and LED 2	$\mathbf{h}_1 + \mathbf{h}_2$	−1	$-RP_t(\mathbf{h}_1 + \mathbf{h}_2) + \mathbf{n}(t)$
01	LED 1	$\mathbf{h}_1$	1	$RP_t\mathbf{h}_1 + \mathbf{n}(t)$
10	LED 2	$\mathbf{h}_2$	1	$RP_t\mathbf{h}_2 + \mathbf{n}(t)$
11	LED 1 and LED 2	$\mathbf{h}_1 + \mathbf{h}_2$	1	$RP_t(\mathbf{h}_1 + \mathbf{h}_2) + \mathbf{n}(t)$

Table 3. LED activation and received signal for two-LED GSSPM system.

where $\gamma_s^{\text{GSPPM}} = E_s^{\text{GSPPM}}/N_0$ is the transmit SNR per GSPPM symbol and $E_s^{\text{GSPPM}} = (RP_t)^2 T_c$ transmit energy of GSSPM symbol. Moreover, using Eq. (25), the average probability of correctly decoding the transmitted pulse position can be expressed as [5]:

$$P_{\text{c, ppm}}^{\text{GSPPM}} = 1 - \left[\frac{1}{2^{N_t}} \sum_{v=1}^{2^{N_t}} \left((L-1) \times Q\left(\|\lambda_v \mathbf{w}_v\|_F \sqrt{\gamma_S^{\text{GSPPM}}} \right) \right) \right] \tag{35}$$

By combining Eqs. (34) and (35), the union bound on the average probability of symbol error of the GSPPM scheme is derived as [5]:

$$
\begin{aligned}
P_{\text{e, sym}}^{\text{GSPPM}} \leq 1 - & \left[1 - \frac{2}{2^{N_t}} \sum_{v=1}^{2^{N_t}-1} \sum_{u=v+1}^{2^{N_t}} Q\left(\|\lambda_v \mathbf{w}_v - \lambda_u \mathbf{w}_u\|_F \sqrt{\frac{\gamma_S^{\text{GSPPM}}}{2}} \right) \right] \\
& \times \left[\frac{(L-1)}{2^{N_t}} \sum_{v=1}^{2^{N_t}} \left(\frac{1}{(L-1)} - Q\left(\|\lambda_v \mathbf{w}_v\|_F \sqrt{\gamma_S^{\text{GSPPM}}} \right) \right) \right]
\end{aligned}
\tag{36}
$$

As shown in **Figure 9**, the closed-form expression for the theoretical SER of GSPPM in Eq. (36) is validated by simulation results. Moreover, the plot also highlights the energy efficiency benefit that PPM adds to GSPPM. As L increases from 2 to 8, the γ_b required to achieve an SER of 10^{-6} reduces by about 2 and 1.5 dB for $N_t = 2$ and $N_t = 4$, respectively.
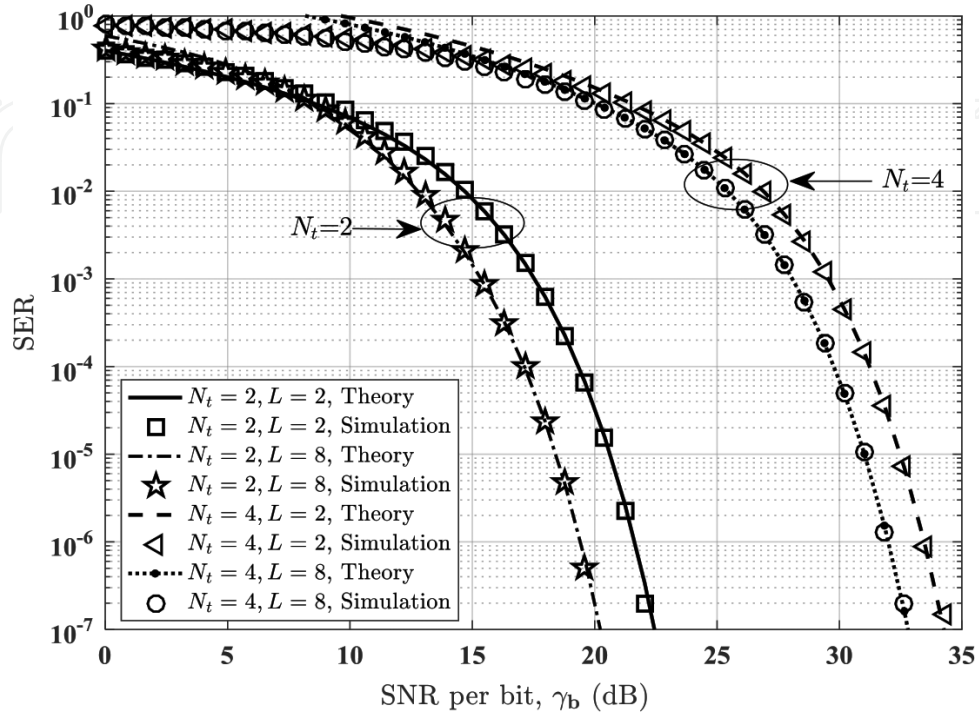

Figure 9. Error performance plot of GSPPM for $N_t = [2, 4]$, $N_r = 1$, and $L = [2, 8]$.
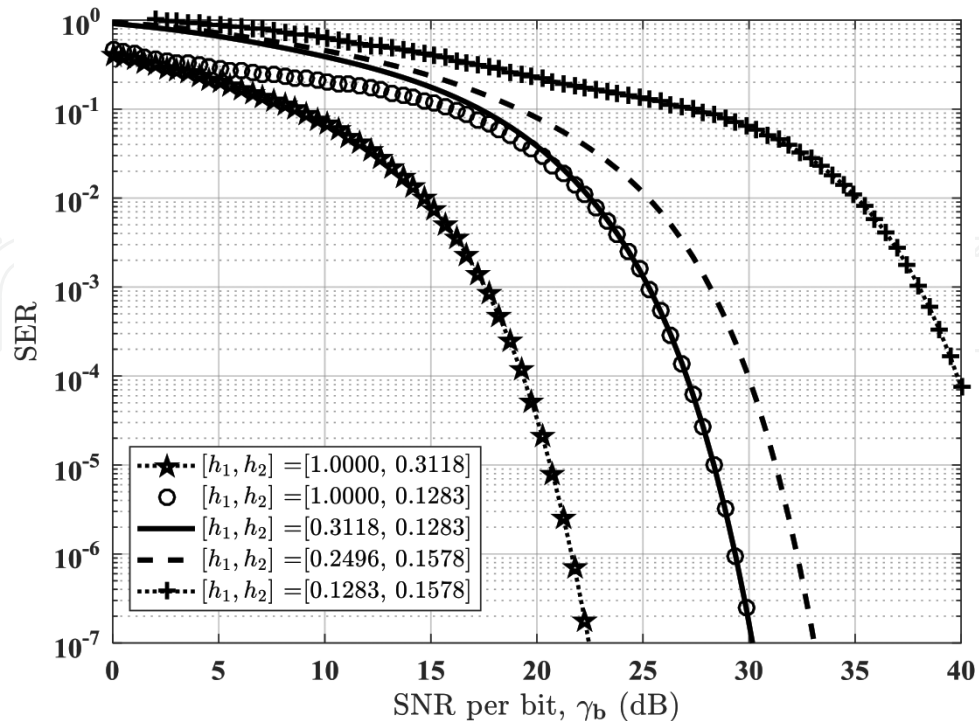

Figure 10. Error performance plot of GSPPM for different channel gains, $N_t = 2$ and $L = 2$.

Using GSPPM as a case study, the impact of channel gains on the performance of optical SM is illustrated in **Figure 10** with the error performance plot for different channel gain values. The plots show that the higher the difference between the channel gains, the lower the SNR required to achieve a given SER. According to Eq. (36), the SER also depends on the absolute value of the channel gains. For instance, to achieve an SER of 10^{-6}, the normalised channel gain $[h_1, h_2] = [1, 0.3118]$ requires about 20 dB less in SNR than the set $[h_1, h_2] = [1, 0.1283]$ even though the channel gain separation $|h_1, h_2|$ for the latter set is higher. Moreover, the effect of the individual channel gain values becomes more significant as SNR increases. This is observed in the case of the normalised channel gain sets $[h_1, h_2] = [1, 0.1283]$ and $[h_1, h_2] = [0.3118, 0.283]$. Both sets require about 29 dB to achieve an SER of 10^{-6}. It can thus be inferred from **Figure 10** that at lower SNR values, the error performance is dictated by the difference in the channel gains and at high SNR by the value of the smaller channel gain.

4. SM comparison with conventional modulation techniques

A performance comparison among different variants of optical SM and other common modulation schemes used for optical wireless communications is shown in **Table 4**. These modulation schemes are compared based on the average transmitted optical power P_{ave}, spectral efficiency η_{spec} and the number of bits per symbol M. These parameters can be obtained from the expressions provided in **Table 4**, where P_t^{modtype} represents the transmitted peak optical power for the stated modulation type 'modtype', and τ is the duty cycle of the modulation schemes that utilise RZ pulse pattern. The spectral efficiency here is defined as the ratio of the bit rate to the bandwidth requirement of the system, where bandwidth requirement is equivalent to the reciprocal of the pulse duration in each of the modulation scheme.

Considering the case of $N_t = 2$ and using the expressions in **Table 4**, the spectral and energy efficiency of the four optical SM schemes analysed in Section 3 are plotted against the number of PPM time slots, L, in **Figures 11** and **12**, respectively. Energy efficiency is expressed in terms of the SNR required to achieve a representative SER of 10^{-6}, and for a fair comparison, all the modulation techniques are assumed to have the same P_{ave} as the GSPPM. For the configuration

Modulation type	P_{ave}	M	η_{spec}
RC RZ-OOK	$\frac{\tau}{2} P_t^{\text{OOK}}$	1	τ
RC L-PPM	$\frac{1}{L} P_t^{\text{PPM}}$	$\log_2 L$	$\frac{1}{L} \log_2 L$
SSK	P_t^{SSK}	$\log_2 N_t$	$\log_2 N_t$
GSSK	$N_t P_t^{\text{GSSK}} \left(\frac{\tau}{2} + \frac{1-\tau}{2^{N_t}} \right)$	N_t	N_t
SPPM	$\frac{P_t^{\text{SPPM}}}{L}$	$\log_2(LN_t)$	$\frac{\log_2(LN_t)}{L}$
GSPPM	$\frac{N_t P_t^{\text{GSPPM}}}{L} \left(\frac{1}{2} + \frac{1}{2^{N_t}} \right)$	$N_t + \log_2 L$	$\frac{N_t + \log_2 L}{L}$

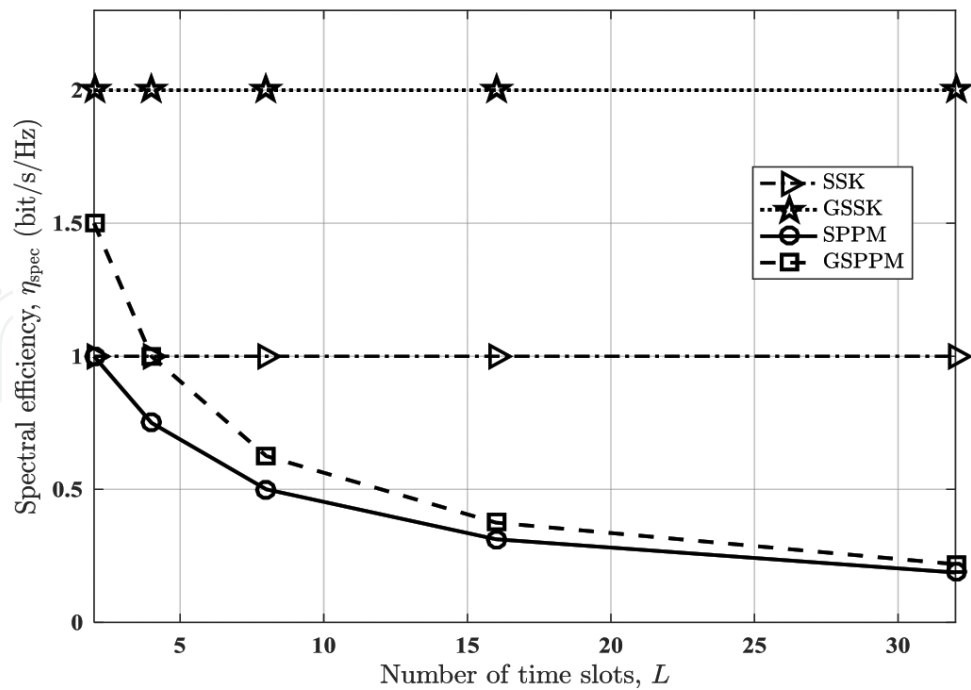**Table 4.** Comparison of optical modulation schemes.

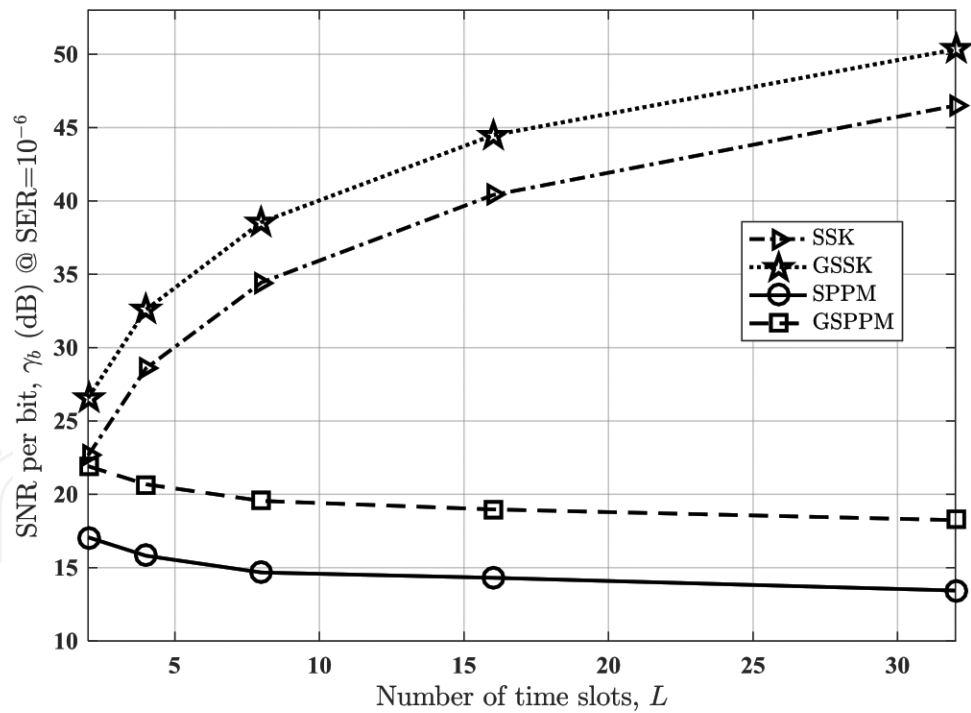**Figure 11.** Spectral efficiency comparison of optical SM schemes.

Figure 12. Energy efficiency comparison of optical SM schemes.

described above, as shown in **Figure 11**, the η_{spec} of GSSK exceeds the maximum achievable values in SSK and SPPM by 1 bits/s/Hz and that of the GSPPM scheme by 0.5 bits/s/Hz. The superiority of GSSK over GSPPM in terms of η_{spec} is because the pulse duration in GSSK is L times longer than that of GSPPM, even though GSPPM transmits more bits/symbol. However, in

terms of energy efficiency, **Figure 12** shows that GSSK and SSK are less energy efficient when compared with SPPM and GSPPM. The SNR requirement of GSSK for $L = 8$ exceeds those of SPPM and GSPPM by up to 23 and 18 dB, respectively. This can be attributed to the energy efficiency benefit that PPM adds to both SPPM and GSPPM.

5. Summary

In this chapter, a detailed description of SM signal generation and detection for VLC systems has been discussed. An overview of different variants of optical SM—OSSK, GSSK, SPPM, S-PAM, and GSM—with their error performance analysis under VLC channel impairments and AWGN has been presented. The analyses of the error performance of these variants have been derived using union bound method and ML criteria. The analytical expressions enabled the theoretical evaluation of the error probability of optical SM technique in a typical MIMO VLC system. Results showed a perfect match between theory and simulations. A summary of the differences between optical SM and other MIMO transmission schemes like SMP, RC, and spatial diversity has also been discussed. The optical SM is thus a technique capable of delivering high data rates in the presence of the limitations of the optical front-end devices. This chapter concludes with the comparison of the spectral and energy efficiency of the variants of optical SM.

Author details

Hammed G. Olanrewaju[1], Funmilayo B. Ogunkoya[2] and Wasiu O. Popoola[1]*

*Address all correspondence to: w.popoola@ed.ac.uk

1 University of Edinburgh, UK

2 Obafemi Awolowo University, Nigeria

References

[1] Mesleh R, Elgala H, Haas H. Optical spatial modulation. Journal of Optical Communications and Networking. 2011;**3**(3):234–244

[2] Mesleh R, Elgala H, Haas H. Spatial modulation. IEEE Transactions on Vehicular Technology. 2008;**57**(4):2228–2241

[3] Ijaz M, Tsonev D, McKendryt JJD, Xiet E, Rajbhandari S, Chun H, et al. Experimental proof-of-concept of optical spatial modulation OFDM using micro LED. In: IEEE Int. Conf. Commun. Work.; IEEE; 2015. pp. 1338–1343

[4] Popoola WO, Poves E, Haas H. Spatial pulse position modulation for optical communications. Journal of Lightwave Technology. 2012;**30**(18):2948–2954

[5] Olanrewaju HG, Thompson J, Popoola WO. Generalized spatial pulse position modulation for optical wireless communications. In: 84th IEEE Vehicular Technology Conference (VTC Fall); IEEE; 2016

[6] Faith T, Di Renzo M, Haas H. On the performance of space shift keying for optical wireless communications. In: IEEE Globecom Workshops; 2010; Miami, FL. IEEE; 2010. pp. 990–994

[7] Fath T, Haas H. Performance comparison of MIMO techniques for optical wireless communications in indoor environments. IEEE Transactions on Communications. 2013;**61** (2):733–742

[8] Popoola WO, Poves E, Haas H. Error performance of generalised space shift keying for indoor visible light communications. IEEE Transactions on Communications. 2013;**61** (5):1968–1976

[9] Fath T, Haas H, Di Renzo M, Mesleh R. Spatial Modulation applied to Optical Wireless Communications in Indoor LOS Environments. In: IEEE Global Telecommunications Conference (GLOBECOM); IEEE; 2011. pp. 1–5

[10] Zhang X, Dimitrov S, Sinanovic S, Haas H. Optimal power allocation in spatial modulation OFDM for visible light communications. In: IEEE 75th Veh. Technol. Conf. (VTC Spring); IEEE; 2012. pp. 1–5

[11] Ghassemlooy Z, Popoola W, Rajbhandari S. Optical Wireless Communications: System and Channel Modelling with MATLAB®. 1st ed. Boca Raton, FL: CRC Press; 2012

[12] Jeganathan J, Ghrayeb A, Szczecinski L, Ceron A. Space shift keying modulation for MIMO channels. IEEE Transactions on Wireless Communications. 2009;**8**(7):3692–3703

[13] Jeganathan J, Ghrayeb A, Szczecinski L. Generalized space shift keying modulation for MIMO channels. In: IEEE 19th Int. Symp. Personal, Indoor and Mobile Radio Commun. (PIMRC); IEEE; 2008. pp. 1–5

[14] Popoola WO, Poves E, Haas H. Demonstration of the merit and limitation of generalised space shift keying for indoor visible light communications. Journal of Lightwave Technology. 2014;**32**(10):1960–1965

[15] Popoola WO, Poves E, Haas H. Generalised space shift keying for visible light communications. In: 8th Int. Symp. Commun. Syst. Networks Digit. Signal Process. (CSNDSP); IEEE; 2012. pp. 1–4

[16] Younis A, Serafimovski N, Mesleh R, Haas H. Generalised spatial modulation. In: 44th Asilomar Conference on Signals, Systems and Computers (ASILOMAR); IEEE; 2010. pp. 1498–1502

[17] Alaka SP, Narasimhan TL, Chockalingam A. Generalized spatial modulation in indoor wireless visible light communication. In: IEEE Global Telecommunications Conference (GLOBECOM); 2015. pp. 1–7

[18] Wang J, Jia S, Song J. Generalised spatial modulation system with multiple active transmit antennas and low complexity detection scheme. IEEE Transactions on Wireless Communications. 2012;**11**(4):1605–1615

[19] Armstrong J. OFDM for optical communications. Journal of Lightwave Technology. 2009;**27**(3):189–204

[20] Barros DJ, Wilson SK, Kahn JM. Comparison of orthogonal frequency-division multiplexing and pulse-amplitude modulation in indoor optical wireless links. IEEE Transactions on Communications. 2012;**60**(1):153–163

[21] Di Renzo M, Haas H, Ghrayeb A, Sugiura S, Hanzo L. Spatial modulation for generalized MIMO: Challenges, opportunities, and implementation. Proceedings of the IEEE. 2014;**102**(1):56–103

[22] Fath T, Haas H. Optical spatial modulation using colour LEDs. In: IEEE International Conference on Communications (ICC); 2013; IEEE; 2013. pp. 3938–3942

[23] Barry JR, Kahn JM, Krause WJ, Lee EA, Messerschmitt DG. Simulation of multipath impulse response for indoor wireless optical channels. IEEE Journal on Selected Areas in Communications. 1993;**11**(3):367–379

[24] Proakis JG, Salehi M. Digital Communications. 5th ed. New York: McGraw-Hill; 2008